Selected papers presented at the XIII All-Polish Seminar on Mössbauer Spectroscopy (OSSM 24)

Magnetic Ordering and Local Atomic Environments in $Na_{0.67}Fe_{1-y}Mn_yO_2$-Cathode Materials for Na-Ion Batteries

R. Idczak[a,*], K. Walczak[b], R. Konieczny[a], P. Sobota[a,c], W. Nowak[a,c] and V.H. Tran[c]

[a]*Institute of Experimental Physics, University of Wrocław, pl. M. Borna 9, 50-204 Wrocław, Poland*
[b]*Faculty of Energy and Fuels, AGH University of Science and Technology, Al. Mickiewicza 30, 30-059 Kraków, Poland*
[c]*Institute of Low Temperature and Structure Research, Polish Academy of Sciences, Okólna 2, 50-422 Wrocław, Poland*

Doi: 10.12693/APhysPolA.146.244 *e-mail: rafal.idczak@uwr.edu.pl

The $Na_{0.67}Fe_{1-y}Mn_yO_2$ ($y = 0.5$ and 0.8) samples were investigated using ^{57}Fe Mössbauer spectroscopy at temperatures ranging from 4.5 to 700 K and superconducting quantum interference device magnetometer at temperatures ranging from 2 to 300 K. It was found that both materials order antiferromagnetically below Néel temperature $T_N = 9.5(5)$ K. Above this temperature, the samples exhibit a local-moment paramagnetism contributed from the Fe^{3+}, Mn^{3+}, and Mn^{4+} ions in high-spin state. The collected temperature-dependent Mössbauer spectra give clear evidence that they cannot be described using one component attributed to the iron atoms, which occupy only one crystallographic position in the hexagonal $P6_3/mmc$ (P2-type) structure. The presence of the second component in all measured transmission Mössbauer spectroscopy spectra is ascribed to the highly distorted FeO_6 octahedra, which are caused by a deficiency of Na atoms in the vicinity of the Mössbauer ^{57}Fe probes. The Debye temperatures $\Theta_D = 554(29)$ K (for $y = 0.5$) and 437(42) K (for $y = 0.8$) were obtained.

topics: Na-ion batteries, Mössbauer spectroscopy, magnetic ordering

1. Introduction

In the last 20 years, rechargeable lithium-ion batteries (LIBs) have become a dominant energy storage technology. Unfortunately, the large-scale demand for lithium associated with the gradually decreasing abundance of this element in the Earth's crust has led to a significant increase in the lithium price. Therefore, there is a critical and urgent need to develop some alternatives for LIBs that will be based on more abundant elements [1–3].

Nowadays, sodium-ion batteries (SIBs) are considered an alternative to LIBs due to the fact that sodium is the fourth most abundant element on earth, and compared with lithium, Na has quite similar physical and chemical properties [2, 3]. Among the various materials studied, sodium-layered oxides (Na_xMO_2, M = transition metal) are a perspective family. The most promising candidates are based on the Mn and Fe elements, which are less expensive ones among the 3*d* elements [4–6].

In our previous work [7], we presented the complex analysis of the structural, transport, and electrochemical properties of $Na_{0.67}Fe_{1-y}Mn_yO_2$ ($y = 0.4$, 0.5, 0.6, 0.7, and 0.8) materials, which crystallize in layered P2-type crystal structure with hexagonal $P6_3/mmc$ space group. In particular, transmission Mössbauer spectroscopy (TMS) studies revealed that only high-spin Fe^{3+} ions are observed in all as-obtained samples (pristine and in various states of sodium intercalation/deintercalation). This finding suggests that only Mn^{3+}/Mn^{4+} ions are involved in electrochemical oxidation/reduction processes in the studied materials. Despite the absence of Fe^{4+} ions in studied samples, the measured room temperature ^{57}Fe Mössbauer spectra of $Na_{0.67}Fe_{1-y}Mn_yO_2$ display an asymmetric shape and cannot be reliably fitted by one symmetric quadrupole-split component (paramagnetic doublet) [7]. This result is rather unexpected, since in the P2-type hexagonal structure of $Na_{0.67}Fe_{1-y}Mn_yO_2$ compounds, the iron atoms occupy only one crystallographic position. Because of that, possible mechanisms of the observed asymmetry should be considered. Three alternatives are: (i) the texture effect (preferred orientation of the electric field gradient at ^{57}Fe nuclei), (ii) the Goldansky–Karyagin effect (an anisotropy of the recoilless fraction), and (iii) the presence of more than one doublet in the recorded spectrum [8, 9].

In this work, in order to select the correct interpretation of Mössbauer data, we performed measurements of Mössbauer spectra of $Na_{0.67}Fe_{1-y}Mn_yO_2$ ($y = 0.5$ and 0.8) samples in the temperature range of 4.2–700 K. Since the recorded at low temperatures TMS spectra reveal that the system undergoes a magnetic transition, we decided to perform additional magnetic measurements down to 2 K. The obtained results give comprehensive information about magnetic ordering and local atomic environments in $Na_{0.67}Fe_{1-y}Mn_yO_2$ compounds.

2. Experimental details

$Na_{0.67}Fe_{1-y}Mn_yO_2$ ($y = 0.5$ and 0.8) powders were obtained by a conventional solid-state reaction with Na_2CO_3 (POCH, 99.8%), $MnCO_3$ (Chempur, $> 99.9\%$), and Fe_2O_3 (POCH, 99%) used as substrates. In order to prevent sodium losses during the synthesis, 5 wt% of Na_2CO_3 excess was added. The raw materials were grounded in a mortar and pelletized into cylindrical pellets with a diameter of 13 mm. The synthesis was performed at 900°C for 12 h in an oxygen atmosphere, followed by fast quenching to room temperature. In the case of $Na_{0.67}Fe_{0.2}Mn_{0.8}O_2$, the temperature of synthesis was reduced to 800°C. This preparation procedure was repeated till obtaining single-phased materials [7].

The collected X-ray diffraction (XRD) patterns for $Na_{0.67}Fe_{1-y}Mn_yO_2$ ($y = 0.5$ and 0.8) powders, which are presented in our previous work [7], indicate that both synthesized materials crystallize in hexagonal $P6_3/mmc$ (P2-type) structure. Reflections that could be ascribed to secondary phases, i.e., rhombohedral $R\bar{3}m$ (O3-type), were not observed.

The ^{57}Fe Mössbauer spectra were recorded in transmission geometry with a conventional constant-acceleration spectrometer. In measurements, a standard ^{57}Co-in-Rh source was used. The sample temperature was controlled using a variable-temperature insert in an Oxford Instruments Spectromag cryostat (in the range of 1.4–300 K) and a standard Mössbauer furnace (in the range of 300–700 K). The collected TMS spectra were analysed using a least-squares fitting procedure, which provides the values of hyperfine interaction parameters such as isomer shift (IS), quadrupole splitting/shift (QS), hyperfine field (B), as well as the relative intensities of the components (C) and the full width at half maximum FWHM (Γ) of spectral lines. All IS values presented in this work are related to the IS value of α-Fe measured at room temperature.

The DC magnetization measurements from 2 to 300 K in various external magnetic fields up to $\mu_0 H = 7$ T were conducted using a superconducting quantum interference device (SQUID) magnetometer (Quantum Design MPMS XL-7). The presented values of mass magnetic susceptibility χ_m and mass magnetization σ have an uncertainty of less than 5%.

3. Results and discussion

The selected TMS spectra of the $Na_{0.67}Fe_{0.5}Mn_{0.5}O_2$ sample measured at various temperatures are presented in Fig. 1. At temperatures between 30 and 700 K, we observe only an asymmetric doublet indicating that the material is in the paramagnetic state. At the same time, the presence of six-line patterns (Zeeman sextets) observed in spectra measured below 10 K reveals that the studied system undergoes a magnetic transition. Fortunately, a visual inspection of Zeeman-split spectra gives clear evidence that they cannot be described by only one component (sextet). Therefore, this finding confirms that the TMS spectra of the $Na_{0.67}Fe_{0.5}Mn_{0.5}O_2$ sample must be described using two components [7].

Taking the above into account, the TMS spectra measured above 10 K were described by two paramagnetic doublets, while the spectra cooled below 10 K were described by two sextets. The relative intensities of these two components are $C_1 = 57\%$ and $C_2 = 43\%$ [7]. The derived IS_1, IS_2, QS_1, and QS_2 parameters are presented in Fig. 2. In general, these values suggest that both components can be ascribed to a high-spin Fe^{+3} state in FeO_6 octahedral environment of hexagonal $P6_3/mmc$ (P2-type) structure. The presence of rhombohedral $R\bar{3}m$ (O3-type) phase is excluded, since the determined QS_1 and QS_2 values are much higher than the expected $QS \approx 0.47$ mm/s for the O3-type phase [10]. For a given temperature, the difference between IS_1 and IS_2 parameters $\Delta IS < 0.02$ mm/s. Therefore, these results indicate that both components can be connected with different local distortions of the FeO_6 octahedra, and the doublet characterized by larger QS_1 values corresponds to highly distorted FeO_6 octahedra, which are caused by a deficiency of Na atoms in the vicinity of the Mössbauer ^{57}Fe probes [7].

As one can notice in Fig. 2a, above 10 K, the values of IS_1 and IS_2 parameters decrease concavely with temperature. As expected, due to the second-order Doppler (SOD) effect [8, 9], the $IS(T)$ dependence could be expressed in terms of the Debye approximation of the lattice vibrations as [9]

$$IS(T) = IS_0 - \frac{9}{2}\frac{k_B T}{cM}\left(\frac{T}{\Theta_D}\right)^3 \int_0^{\Theta_D/T} \frac{\mathrm{d}x\, x^3}{\mathrm{e}^x - 1}, \quad (1)$$

where IS_0 stands for the chemical isomer shift, which is temperature-independent, k_B is the Boltzmann constant, M denotes the mass of ^{57}Fe, c is the

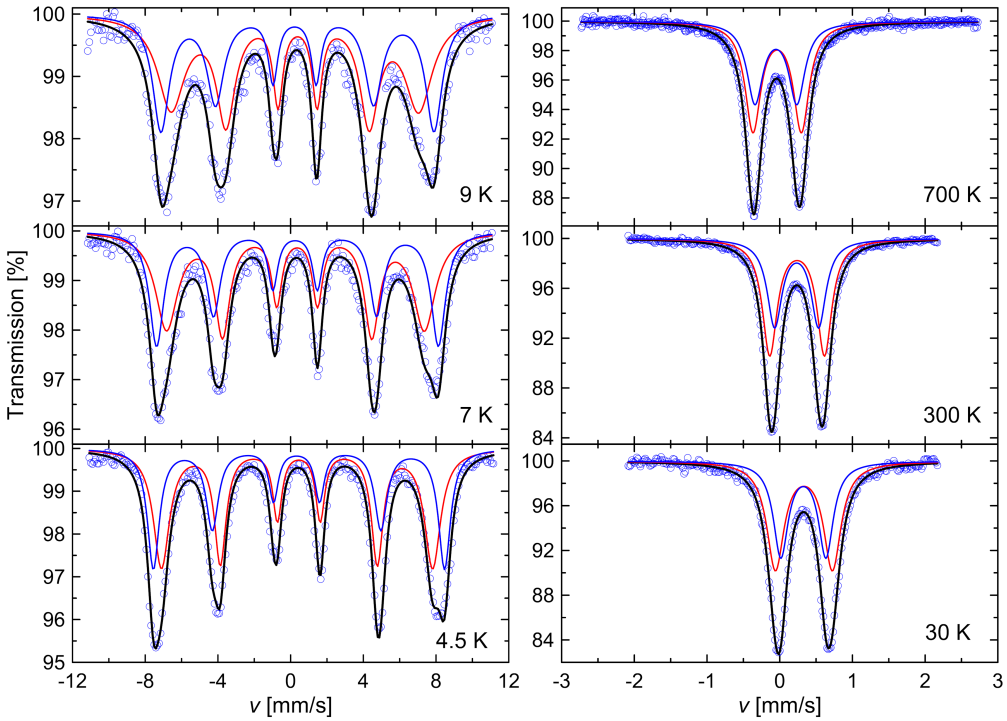

Fig. 1. The selected TMS spectra of $Na_{0.67}Fe_{0.5}Mn_{0.5}O_2$ sample measured at various temperatures. All spectra were described using two components (red and blue lines); see text.

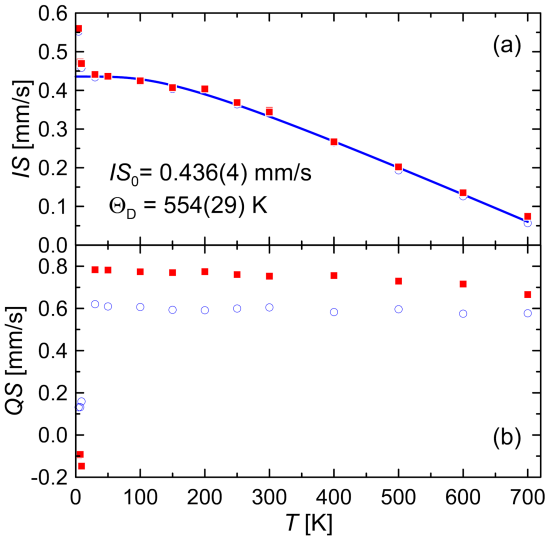

Fig. 2. (a) The temperature dependence of IS_1 (red points) and IS_2 (blue points) parameters derived from TMS spectra measured for $Na_{0.67}Fe_{0.5}Mn_{0.5}O_2$. The solid line represents the fit of experimental IS values to (1). (b) The temperature dependence of QS_1 (red points) and QS_2 (blue points) parameters. The standard uncertainties for the presented quantities do not exceed 2%.

speed of light in vacuum, and Θ_D denotes the Debye temperature. Fitting experimental data to (1) yields $IS_0 = 0.436(4)$ mm/s and $\Theta_D = 554(29)$ K.

The temperature dependencies of QS_1 and QS_2 parameters between 30 and 700 K, which are presented in Fig. 2b, show that both parameters slightly decrease with temperature. A similar behavior was observed in many metallic systems [11–13], indicating that in this temperature range, no structural phase transition is observed. The spectral line widths do not vary with temperature and are close to $\Gamma_1 = 0.26(1)$ mm/s and $\Gamma_2 = 0.24(1)$ mm/s.

Below 10 K, the measured spectra change significantly, revealing that the $Na_{0.67}Fe_{0.5}Mn_{0.5}O_2$ compound undergoes the magnetic transition. As one can see in Fig. 1, the spectra were well-fitted by two sextets. The component which is attributed to the highly distorted FeO_6 octahedra exhibits broad lines and hyperfine fields $B_1 = 42.2(2)$ T, 44.0(1) T, and 46.2(1) T at 9 K, 7 K, and 4.5 K, respectively. The broadening of the spectral lines can be attributed to magnetic relaxation effects [9] as well as to a distribution of magnetic environments caused by the local lattice distortion around iron atoms [13, 14]. The second sextet with more narrow lines and higher hyperfine fields $B_2 = 46.6(1)$ T, 48.0(1) T, and 49.6(1) T at 9 K, 7 K, and 4.5 K, respectively, is ascribed to undistorted FeO_6 octahedra. The observed relatively high values of hyperfine fields are comparable with those reported for antiferromagnetic ordered α-$NaFeO_2$ ($B = 45.5$ T at 4.2 K) [15] and $LiFeO_2$ ($B = 48.3$ T at 4 K) [16]. At the same time, below 10 K, the determined isomer shift values rapidly increase while quadrupole

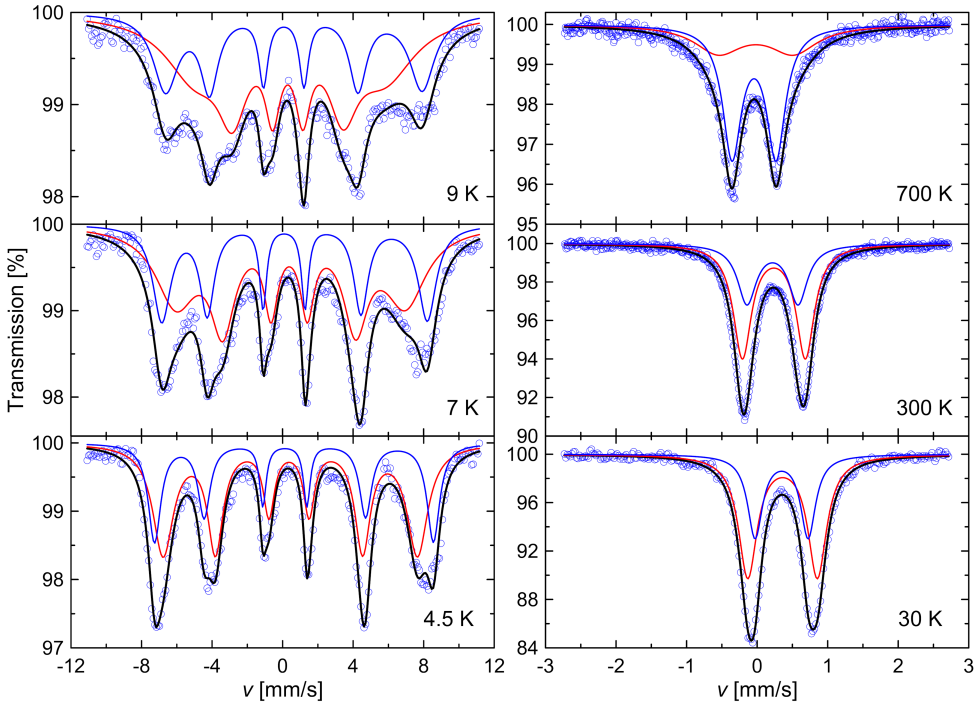

Fig. 3. The selected TMS spectra of $Na_{0.67}Fe_{0.2}Mn_{0.8}O_2$ sample measured at various temperatures. All spectra were described using two components (red and blue lines); see text.

shifts rapidly decrease with lowering temperature. This finding indicates that the electronic structure of $Na_{0.67}Fe_{0.5}Mn_{0.5}O_2$ compound in a paramagnetic state changes significantly due to the magnetic transition. In particular, the observed rapid increase in IS parameter with lowering temperature (from 30 to 4.5 K) may be related to the effect of the magnetism on lattice vibrations [17]. Additionally, using the QS values determined for the paramagnetic state at 30 K and the magnetic state at 4.5 K, we can determine the angle φ between the direction of the internal magnetic field and the principal axis of the electric field gradient (EFG). Using QS values obtained for the component ascribed to undistorted FeO_6 octahedra and the equation [18–20]

$$QS_{\mathrm{mag}} = \frac{1}{2} QS_{\mathrm{para}} \left(3\cos^2(\varphi) - 1\right), \qquad (2)$$

we obtain $\varphi = 46(2)^\circ$.

The selected TMS spectra of $Na_{0.67}Fe_{0.2}Mn_{0.8}O_2$ sample measured at various temperatures are presented in Fig. 3. The collected spectra are described similarly to those obtained for $Na_{0.67}Fe_{0.5}Mn_{0.5}O_2$, using two doublets at temperatures between 30 and 700 K ($\Gamma_1 = 0.30(1)$ mm/s and $\Gamma_2 = 0.26(2)$ mm/s) and two sextets, with broadened spectral lines, below 30 K.

The derived IS_1, IS_2, QS_1, and QS_2 parameters are presented in Fig. 4. First, it should be noted that at temperatures between 4.5 and 500 K, the relative intensities of two components are $C_1 = 65\%$ and $C_2 = 35\%$. As it was mentioned in work [7], this result could be explained by assuming that Na ions accumulate mostly around Mn atoms. As a result, the increase in Mn content in the $Na_{0.67}Fe_{1-y}Mn_yO_2$ system generates an additional number of highly distorted FeO_6 octahedra, which leads to a systematic increase in the C_1 parameter. However, above 500 K, C_1 decreases with temperature, and at 700 K, $C_1 < C_2$. This indicates that the Lamb–Mössbauer factor of Fe^{+3} ions located in the distorted FeO_6 octahedra suddenly decreases. At the same time, the values of Γ_1 and QS_1 parameters strongly increase at 600 K ($\Gamma_1 = 0.61(7)$ mm/s, $QS_1 = 0.94(3)$ mm/s) and 700 K ($\Gamma_1 = 0.78(4)$ mm/s, $QS_1 = 1.19(3)$ mm/s). All these changes are probably caused by a high diffusivity of O and Fe ions in distorted FeO_6 octahedra at temperatures above 500 K. Similar effects were observed in various materials at temperatures close to their melting point [21, 22]. Since this effect is not observed in $Na_{0.67}Fe_{0.5}Mn_{0.5}O_2$, it seems that the $Na_{0.67}Fe_{0.2}Mn_{0.8}O_2$ compound is less thermally stable.

The $IS_2(T)$ dependence between 30 and 700 K can be described using (1), yielding $IS_0 = 0.457(7)$ mm/s and $\Theta_{\mathrm{D}} = 437(42)$ K (see Fig. 4). Comparison of this result with $\Theta_{\mathrm{D}} = 554(29)$ K, calculated for $Na_{0.67}Fe_{0.5}Mn_{0.5}O_2$, suggests that Θ_{D} decreases with increasing Mn content in $Na_{0.67}Fe_{1-y}Mn_yO_2$ system.

Below 10 K, the measured TMS spectra reveal the presence of two sextets. Similarly to results for $Na_{0.67}Fe_{0.5}Mn_{0.5}O_2$, the first component which exhibits broad lines and hyperfine fields

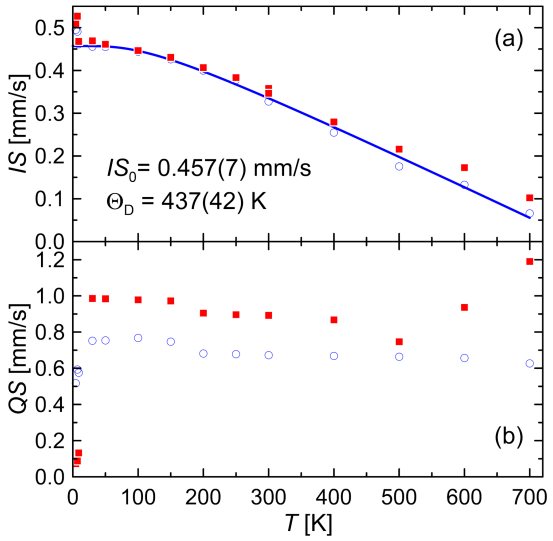

Fig. 4. (a) The temperature dependence of IS_1 (red points) and IS_2 (blue points) parameters derived from TMS spectra measured for $Na_{0.67}Fe_{0.2}Mn_{0.8}O_2$. The solid line represents the fit of experimental IS_2 values to (1). (b) The temperature dependence of QS_1 (red points) and QS_2 (blue points) parameters. The standard uncertainties for the presented quantities do not exceed 4%.

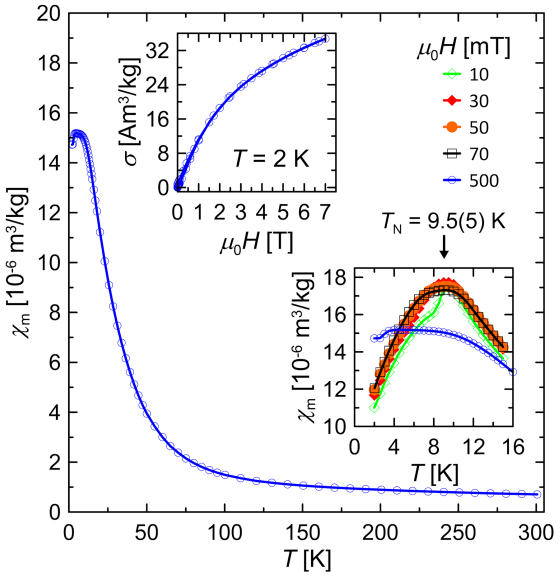

Fig. 5. The temperature dependence of the mass susceptibility measured in a field of $\mu_0 H = 0.5$ T for $Na_{0.67}Fe_{0.5}Mn_{0.5}O_2$. The upper inset presents mass magnetization versus applied fields at $T = 2$ K; the lower inset presents $\chi_m(T)$ data at low temperatures.

$B_1 = 33.5(3)$ T at 9 K, 40.3(3) T at 7 K and 44.7(1) T at 4.5 K, is ascribed to the highly distorted FeO_6 octahedra. The second sextet with more narrow lines and $B_2 = 45.1(1)$ T, 46.6(1) T, and 48.0(1) T at 9 K, 7 K, and 4.5 K, respectively, is attributed to undistorted FeO_6 octahedra. The determined values of B_1 and B_2 for this sample are lower than the corresponding values obtained for $Na_{0.67}Fe_{0.5}Mn_{0.5}O_2$. This finding can be related to the fact that in both studied materials, three types of magnetic ions exist. According to work [7], these ions are the high-spin Fe^{3+}, Mn^{3+}, and Mn^{4+}. Since the effective magnetic moment μ_{eff} of free Fe^{3+} is equal to $5.92\mu_B$, while $\mu_{\text{eff}} = 4.9\mu_B$ for Mn^{3+} and $\mu_{\text{eff}} = 3.87\mu_B$ for Mn^{4+}, the decrease in B_1 and B_2 values with increasing Mn content in $Na_{0.67}Fe_{1-y}Mn_yO_2$ system is expected.

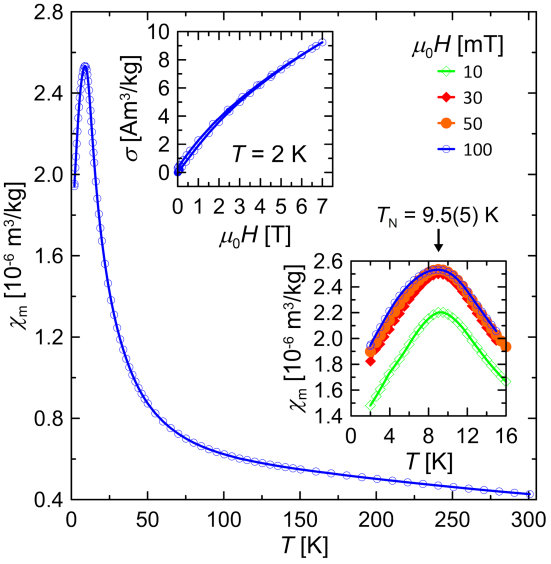

Fig. 6. The temperature dependence of the mass susceptibility measured in a field of $\mu_0 H = 0.1$ T for $Na_{0.67}Fe_{0.2}Mn_{0.8}O_2$. The upper inset presents mass magnetization versus applied fields at $T = 2$ K; the lower inset presents $\chi_m(T)$ data at low temperatures.

The temperature dependence of the mass susceptibility measured in a field of $\mu_0 H = 0.5$ T for $Na_{0.67}Fe_{0.5}Mn_{0.5}O_2$ is presented in Fig. 5. The behavior of $\chi_m(T)$ between 10 and 300 K indicates a local-moment paramagnetism contributed from the Fe^{3+}, Mn^{3+}, and Mn^{4+} ions in the high-spin state. Below 10 K, the $\chi_m(T)$ values start to decrease with lowering temperatures revealing that the sample undergoes the antiferromagnetic transition at Néel temperature $T_N = 9.5(5)$ K. Since, from the TMS spectra measured at $T \leq 9$ K, one cannot distinguish between ferromagnetic and antiferromagnetic ordering, the obtained $\chi_m(T)$ data give clear evidence that the magnetic ordering in the studied sample is of antiferromagnetic type. The $\sigma(H)$ curve measured at 2 K displays no saturation within the range of $\mu_0 H$ from 0 to 7 T. Since the Mössbauer spectrum collected at 4.5 K consists of two sextets with $B_1 = 46.2(1)$ T and $B_2 = 49.6(1)$ T, this result is expected.

The magnetic properties of $Na_{0.67}Fe_{0.2}Mn_{0.8}O_2$, which are presented in Fig. 6, are comparable with those obtained for $Na_{0.67}Fe_{0.5}Mn_{0.5}O_2$. The system is in a paramagnetic state between 10 K and 300 K and undergoes the antiferromagnetic transition below 9.5(5) K. Again, this result is in agreement with TMS data. Note that T_N is similar for both studied samples, indicating that the Mn content in the $Na_{0.67}Fe_{1-y}Mn_yO_2$ system does not have an influence on the antiferromagnetic transition temperature.

4. Conclusions

The magnetic ordering and local atomic environments in $Na_{0.67}Fe_{0.5}Mn_{0.5}O_2$ and $Na_{0.67}Fe_{0.2}Mn_{0.8}O_2$ compounds were studied using TMS in the temperature range of 4.5–700 K and SQUID magnetometer between 2 and 300 K.

The obtained results indicate that both materials undergo the antiferromagnetic transition at $T_N = 9.5(5)$ K. Above T_N, the samples exhibit Curie–Weiss paramagnetism due to the presence of well-localized magnetic moments carried on the Fe^{3+}, Mn^{3+}, and Mn^{4+} ions in the high-spin state.

The analysis of the temperature-dependent Mössbauer spectra reveals that they cannot be described by one component related to the iron atoms, which occupy only one crystallographic position in the hexagonal $P6_3/mmc$ (P2-type) structure. As was shown, all collected TMS spectra contain two components that can be ascribed to different local distortions of the FeO_6 octahedra. The occurrence of the second component may be related to the presence of highly distorted FeO_6 octahedra, which are caused by a deficiency of Na atoms in the vicinity of the ^{57}Fe atoms.

References

[1] B. Dunn, H. Kamath, J.-M. Tarascon, *Science* **334**, 928 (2011).

[2] J.-Y. Hwang, S.-T. Myung, Y.-K. Sun, *Chem. Soc. Rev.* **46**, 3529 (2017).

[3] K. Chayambuka, G. Mulder, D.L. Danilov, P.H.L. Notten, *Adv. Energy Mater.* **10**, 2001310 (2020).

[4] N. Yabuuchi, M. Kajiyama, J. Iwatate, H. Nishikawa, S. Hitomi, R. Okuyama, R. Usui, Y. Yamada, S. Komaba, *Nat. Mater.* **11**, 512 (2012).

[5] G. Singh, B. Acebedo, M.C. Cabanas, D. Shanmukaraj, M. Armand, T. Rojo, *Electrochem. Commun.* **37**, 61 (2013).

[6] W.M. Dose, N. Sharma, J.C. Pramudita, M. Avdeev, E. Gonzalo, T. Rojo, *Chem. Mater.* **30**, 7503 (2018).

[7] K. Walczak, K. Redel, R. Idczak et al., *Energy Technol.* **10**, 2101105 (2022).

[8] N. Greenwood, T. Gibb, *Mössbauer Spectroscopy*, John Wiley & Sons, 1971.

[9] P. Gütlich, E. Bill, A. Trautwein, *Mössbauer Spectroscopy and Transition Metal Chemistry: Fundamentals and Applications*, Springer, Berlin 2010.

[10] E. Lee, D.E. Brown, E.E. Alp, Y. Ren, J. Lu, J.-J. Woo, C.S. Johnson, *Chem. Mater.* **27**, 6755 (2015).

[11] Z.M. Stadnik, P. Wang, H.-D. Wang, C.-H. Dong, M.-H. Fang, *J. Alloys Compd.* **561**, 82 (2013).

[12] M.A. Albedah, F. Nejadsattari, Z.M. Stadnik, J. Przewoźnik, *J. Alloys Compd.* **619**, 839 (2015).

[13] R. Idczak, V. Tran, B. Świątek-Tran, K. Walczak, W. Zając, J. Molenda, *J. Magn. Magn. Mater.* **491**, 165602 (2019).

[14] R. Idczak, B. Kaśków, R. Konieczny, J. Chojcan, *Physica B* **577**, 411794 (2020).

[15] T. Ichida, T. Shinjo, Y. Bando, T. Takada, *J. Phys. Soc. Jpn.* **29**, 795 (1970).

[16] T. Shirane, R. Kanno, Y. Kawamoto, Y. Takeda, M. Takano, T. Kamiyama, F. Izumi, *Solid State Ionics* **79**, 227 (1995).

[17] S.M. Dubiel, *J. Magn. Magn. Mater.* **561**, 169688 (2022).

[18] M.S. Henriques, D.I. Gorbunov, J.C. Waerenborgh, M. Pasturel, A.V. Andreev, M. Dušek, Y. Skourski, L. Havela, A.P. Gonçalves, *Inorg. Chem.* **54**, 9646 (2015).

[19] G. Filoti, M.D. Kuz'min, and J. Bartolomé, *Phys. Rev. B* **74**, 134420 (2006).

[20] R. Idczak, M. Babij, P. Sobota, W. Nowak, R. Konieczny, Z. Bukowski, V. Tran, *J. Magn. Magn. Mater.* **560**, 169676 (2022).

[21] A.J.F. Boyle, D.S.P. Bunbury, C. Edwards, H.E. Hall, *Proc. Phys. Soc.* **77**, 129 (1961).

[22] A. Heiming, K.H. Steinmetz, G. Vogl, Y. Yoshida, *J. Phys. F Metal Phys.* **18**, 1491 (1988).